ChemPubSoc Europe

DOI: 10.1002/cmdc.201600224

CHEMMEDCHEM Communications

Discovery of a Nanomolar Multikinase Inhibitor (KST016366): A New Benzothiazole Derivative with Remarkable Broad-Spectrum Antiproliferative Activity

Ashraf Kareem El-Damasy,[a, b, c] Nam-Chul Cho,[a] Ghilsoo Nam,[a, b] Ae Nim Pae,[a, b] and Gyochang Keum*[a, b]

Herein we report the discovery of compound **6** [KST016366; 4-((2-(3-(4-((4-ethylpiperazin-1-yl)methyl)-3-(trifluoromethyl)phenyl)ureido)benzo[*d*]thiazol-6-yl)oxy)picolinamide] as a new potent multikinase inhibitor through minor structural modification of our previously reported RAF kinase inhibitor **A**. In vitro anticancer evaluation of **6** showed substantial broad-spectrum antiproliferative activity against 60 human cancer cell lines. In particular, it showed GI_{50} values of 51.4 and 19 nM against leukemia K-562 and colon carcinoma KM12 cell lines, respectively. Kinase screening of compound **6** revealed its nanomolar-level inhibitory activity of certain oncogenic kinases implicated in both tumorigenesis and angiogenesis. Interestingly, **6** displays IC_{50} values of 0.82, 3.81, and 53 nM toward Tie2, TrkA, and ABL-1 (wild-type and T315I mutant) kinases, respectively. Moreover, **6** is orally bioavailable with a favorable in vivo pharmacokinetic profile. Compound **6** may serve as a promising candidate for further development of potent anticancer chemotherapeutics.

Cancer is still a prime leading cause of mortality worldwide, accounting for 8.2 million deaths in 2012.[1] Cancer reflects a multistep process, arising from accumulation of hereditary and/or acquired disorders in genes involved in the regulation of cell propagation and survival. Activation or inactivation of four or five different genes may be needed for the development of a clinically detectable human cancer.[2] The conventional cytotoxic chemotherapeutics that directly interact with DNA are one of the cornerstones for cancer treatment. However, their severe side effects constitute a major obstacle that impedes their efficacy. Over the past two decades, the attention of anticancer drug development has shifted dramatically from classical cytotoxic drugs to targeted agents that modulate protein kinases whose activities are more specifically linked with cancerous cells.[3]

In solid tumors, it is unusual for a single kinase aberration to be the sole cause of disease and it is improbable that tumors are dependent on only one dysregulated signaling pathway.[4] In this regard, inhibition of a single kinase may not be sufficient to achieve a clinical benefit, due to either the built-in redundancy of signaling pathways, or the ability of tumors to acquire resistance.[5,6] Therefore, multikinase Inhibitors have emerged as a new paradigm in drug discovery to overcome the resistance arising from selective kinase inhibitors.[7,8] Currently, a number of multitargeted kinase inhibitors are commercially launched.

The absolute majority of kinase inhibitors are known as type I inhibitors, which target the ATP-site of the kinase in its active state (DFG-in). In contrast, type II inhibitors trap their target kinases in the inactive (DFG-out) conformation, occupying a hydrophobic pocket adjacent to the ATP binding site.[9] Sorafenib (Nexavar®) is a multikinase type II inhibitor approved by the Food and Drug Administration (FDA) for treatment of advanced renal carcinoma.[10] Structural analysis of the co-crystal structure of sorafenib[11] and other type II kinase inhibitors[12,13] with their kinases (BRAF, c-KIT and ABL) defined the prerequisite structural features to access type II binding conformation.[14] Accordingly, sorafenib structure could be dissected into the head pyridine moiety as hinge region binder, central phenyl ring linker, urea as hydrogen bond donor/acceptor pair, and a hydrophobic tail (4-chloro-3-trifluoromethylphenyl terminal) that access the hydrophobic pocket created by the flip of the DFG motif of the kinase activation loop.[15]

Recently, we reported a series of 2-ureidoquinolines[16] and ureidobenzothiazoles[17] derivatives as sorafenib congeners by replacing the central phenyl linker of sorafenib with either quinolone[16] or benzothiazole[17] scaffold, while conserving the other structural features. Interestingly, such modifications led to considerable improvement in the cellular anticancer potency as well as favorable inhibitory activity toward B-Raf^{V600E} and C-Raf kinases.

In the present study, we aimed at performing further structural modifications in terms of the hydrophobic tail, in an attempt to improve the anticancer activity of the ureidobenzothiazole **A**.[17] We thought that replacing the small lipophilic chlorine atom of **A** with either (morpholin-1-yl)methyl **5** or (4-ethylpiperazin-1-yl)methyl moiety **6** (Figure 1) may improve the physicochemical properties of compound **A** and hence its

[a] A. K. El-Damasy, Dr. N.-C. Cho, Prof. G. Nam, Prof. A. N. Pae, Prof. G. Keum
Center for Neuro-Medicine, Brain Science Institute,
Korea Institute of Science and Technology (KIST),
Hwarangro 14-gil 5, Seongbuk-gu, Seoul 136-791 (Republic of Korea)
E-mail: gkeum@kist.re.kr

[b] A. K. El-Damasy, Prof. G. Nam, Prof. A. N. Pae, Prof. G. Keum
Department of Biological Chemistry,
Korea University of Science and Technology (UST),
Gajungro 217, Youseong-gu, Daejeon 305-350 (Republic of Korea)

[c] A. K. El-Damasy
Department of Medicinal Chemistry,
Faculty of Pharmacy, University of Mansoura, Mansoura 35516 (Egypt)

Supporting information (detailed procedures for synthesis, cellular and biochemical assays, and molecular docking) and the ORCID identification number(s) for the author(s) of this article can be found under http://dx.doi.org/10.1002/cmdc.201600224.

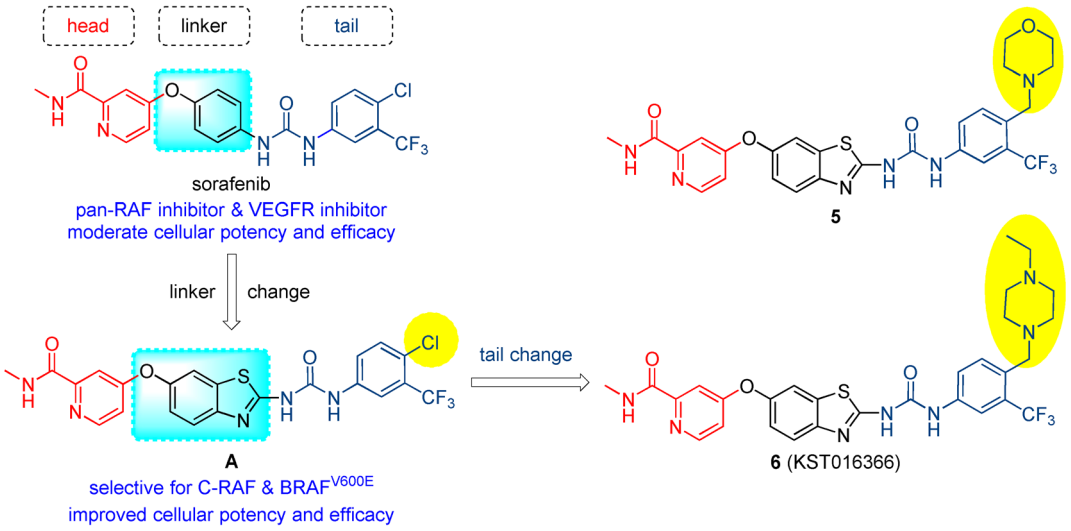

Figure 1. Rational design of the target compounds.

cellular potency. From another perspective, it was worthy to investigate the impact of structural extension in the hydrophobic tail fragment on the affinity toward various protein kinases. In the light of these considerations, two new benzothiazoles **5** and **6** have been designed, synthesized, and evaluated for their anticancer activities over a panel of 60 human cancer cell lines. Moreover, the most promising compound **6** was further tested against a panel of 50 oncogenic kinases.

As illustrated in Scheme 1, in order to prepare the target compounds, we synthesized the two main building blocks **3a**, **3b** and **4**.[17,18] The anilines **3a** and **3b** were prepared in three steps. First, α-bromination of 1-methyl-4-nitro-2-(trifluoromethyl)benzene with *N*-bromosuccinimide (NBS) in the presence of azobisisobutyronitrile (AIBN) afforded the corresponding bromo derivative **1** in 63% yield.[19] Nucleophilic substitution of **1** with morpholine or 4-ethylpiperazine using K_2CO_3 as a base in dichloromethane produced the alkylated nitro derivatives **2a** and **2b**, which underwent reduction with Pd/C under hydrogen atmosphere to yield the corresponding anilines **3a** and **3b**. On the other hand, the 2-aminobenzothiazole derivative **4** was prepared adopting our previously reported method.[17,18] Treatment of the benzothiazol-2-yl amine **4** with 1,1′-carbonyldiimidazole (CDI) in DMF at room temperature produced the corresponding isocyanate. In the same pot, the appropriate aniline **3a** or **3b** was added and the reaction mixture was heated at 100 °C for 3 h to afford the desired ureidobenzothiazoles **5** and **6**.

The antiproliferative activity of compounds **5** and **6** was assessed at 10 μM concentration against a panel of 60 human cancer cell lines at National Cancer Institute (NCI, USA).[20] The mean growth percentage (GP) and growth inhibition (GI) for the full panel cell lines are presented in Table 1.

By referring to the total number of sensitive cells, it could be observed that all the tested compounds possess significant broad spectrum antiproliferative activities (≥53 cell lines). Replacing the lipophilic chlorine group of compound **A** with hy-

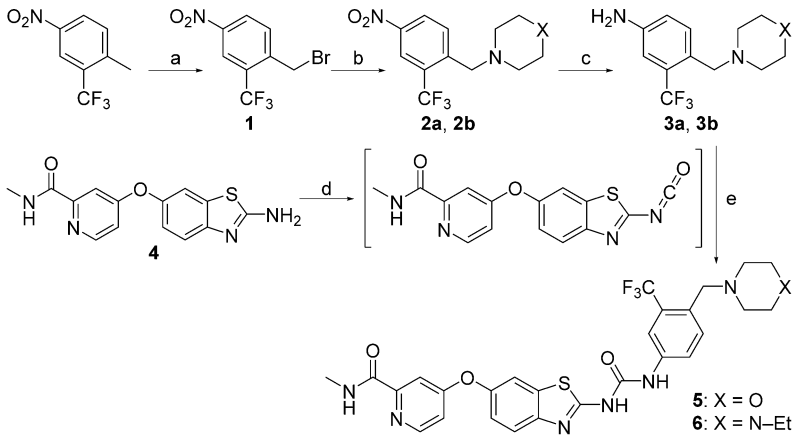

Scheme 1. *Regents and conditions*: a) NBS, AIBN, 1,2-dichloroethane, 90 °C, 18 h, 63%; b) morpholine or 4-ethylpiperazine, K_2CO_3, CH_2Cl_2, RT, 3 h; c) H_2, Pd/C, methanol, RT, 18 h, 99% (X = O, **3a**), 78% (X = N–Et, **3b**), over two steps; d) CDI, DMF, 24 h; e) DMF, 100 °C, 3 h, 16.5% (X = O, **5**), 16.2% (X = N–Et, **6**), over two steps.

Table 1. Molar refractivity (MR) and cLog*P* values of compounds **A**, **5** and **6**, and an overview of their preliminary anticancer assay results at a single-dose concentration of 10 μM.

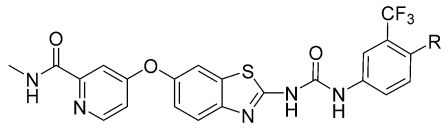

A **5** **6**

R	Cl	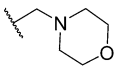	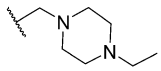
MR [$cm^3 mol^{-1}$]	122.86	146.46	158.40
cLog*P*[a]	5.96	5.17	6.27
Mean growth [%][b]	8.49 ± 30.5	19.9 ± 19.9	−44.6 ± 31.6
Mean growth inhib. [%][b]	91.51 ± 30.4	80.13 ± 21.9	144.6 ± 29.5
Positive cytostatic effect[c]	33/59	51/58	5/53
Positive cytotoxic effect[d]	21/59	5/58	48/53
No. sensitive cell lines	54/59	56/58	53/53

[a] Calculated partition coefficient; values were calculated by ChemDraw Professional 15.0 software. [b] Data were obtained from the NCI in vitro disease-oriented human tumor cell line screen (single-dose mean graph); values were calculated and are presented as the mean ± SD of 60 cell lines. [c] Ratio of the number of cell lines with 0–50% growth over the total number of cell lines. [d] Ratio of the number of cell lines with < 0% growth over the total number of cell lines.

drophilic morpholinomethyl moiety (compound **5**) led to slight decrease in the overall growth inhibitory activity (**A**, GP = 8.49; **5**, GP = 19.9). Interestingly, incorporation of the (4-ethylpiperazin-1-yl)methyl moiety at *para* position neighboring to the *m*-trifluoromethyl group led to remarkable improvement in the activity (**6**, GP = −44.6). Furthermore, and in a stark contrast to the cytostatic activity of compound **5** (51 out of 58), the corresponding ethylpiperazine derivative **6** displayed a distinct positive cytotoxic effect (48 out of 53). In terms of MR, a steric factor parameter, and the lipophilicity indicator cLog*P*, we can observe that increasing both the lipophilic and steric character of the compound, as in **6**, is associated with significant increase in the anticancer activity. The aforementioned findings point out the preponderance of ethylpiperazine than morpholine for achieving excellent antineoplastic activity. The GP of NCI 60 cell lines upon treatment with compounds **5** and **6** as well as the lead compound **A** at 10 μM are shown in Figure 2.

Inspection of the results illustrated in Figure 2 discloses the similar anticancer activity of both the lead compound **A** and its corresponding morpholinomethyl analogue **5**. Moreover, the sound lethal effects of compound **6** (minus values of GP) over numerous hematological and solid cancer cell lines was observed. Of special interest, compound **6** exerted GP = −60.0 against 24 cell lines. The melanoma UACC-62 cell line was the most susceptible cell (GP = −93.0). Based on the impressive antiproliferative activity of both compounds **5** and **6**, they were further evaluated in five-dose testing mode to determine their GI_{50} (the molar concentration causing 50% GI), TGI (the molar concentration producing 100% GI) and LC_{50} (the molar concentration causing 50% lethality or tumor regression). The GI_{50} values, as a measure of compounds' potency, of these two compounds along with the lead compound **A** and sorafenib[21] are listed in Table 2.

As presented in Table 2, compounds **5** and **6** displayed significant potency over almost all of the tested cell lines with sub-micromolar or single-digit micromolar GI_{50} values. Upon comparison with the lead candidate **A**, both **5** and **6** exhibited superior potencies against 24 and 41 various cell lines, respectively. Moreover, compounds **5** and **6** surpassed the antiproliferative activity of sorafenib over 36 and 51 cancer cell lines, respectively. In particular, the morpholine derivative **5** and its ethylpiperazine analogue **6** exerted outstanding potency against the colorectal carcinoma KM12 cell line (**5**, GI_{50} = 446 nM; **6**, GI_{50} = 19 nM), being 7.6 and 179.5-fold, respectively, more potent than the chloro derivative **A** (GI_{50} = 3410 nM). Moreover, compound **6** showed a great growth inhibitory activity toward the leukemia CCRF-CEM and K-562 cell lines with GI_{50} values of 443 and 51.4 nM, respectively.

Apart from potency, the efficacies of **5** and **6** against certain sensitive cell lines were examined and compared with those of the lead compound **A** and sorafenib (Table 3). The high efficacy

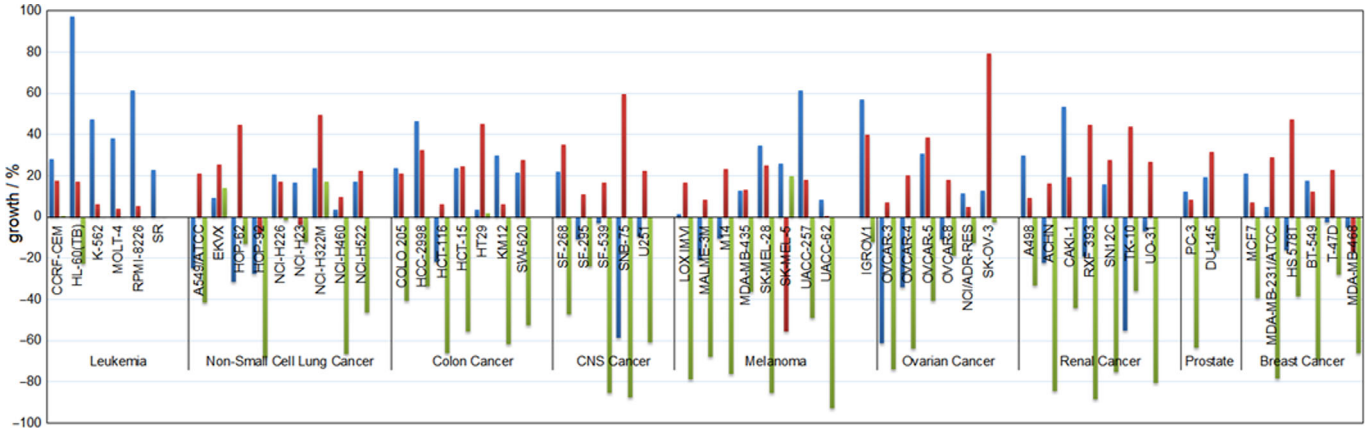

Figure 2. Percent growth of the NCI 60-cell-line panel after treatment with compounds **A** (blue), **5** (red), and **6** (green) at 10 μM.

Table 2. GI_{50} values of compounds **A**, **5**, **6**, and sorafenib over the NCI 60-cell-line panel.[a,b]

Cell line	GI_{50} [μM]				Cell line	GI_{50} [μM]			
	A	**5**	**6**	sorafenib		**A**	**5**	**6**	sorafenib
Leukemia					M14	1.96	2.48	**1.75**	2.00
CCRF-CEM	ND[c]	2.73	***0.443***	2.00	MDA-MB-435	1.90	**1.83**	**1.44**	1.58
HL-60(TB)	> 100	**2.70**	**2.01**	1.58	SK-MEL-2	5.69	**2.74**	**1.75**	2.00
K-562	ND[c]	1.53	***0.051***	3.16	SK-MEL-28	1.56	1.80	**1.24**	2.51
MOLT-4	ND[c]	2.57	2.13	3.16	SK-MEL-5	ND	1.01	1.52	1.58
RPMI-8226	2.22	**1.72**	**2.10**	1.58	UACC-257	3.37	**2.16**	**1.86**	2.00
SR	0.412	1.90	2.81	3.16	UACC-62	2.06	**1.44**	**1.70**	1.58
Non-Small Cell Lung (NSCL) Cancer					**Ovarian Cancer**				
A549/ATCC	1.93	2.15	1.99	3.16	IGROV1	2.02	2.77	**1.76**	2.51
EKVX	1.75	2.10	2.01	2.51	OVCAR-3	2.11	**1.79**	**1.89**	3.16
HOP-62	1.94	2.82	1.95	2.00	OVCAR-4	1.59	1.72	1.69	3.16
HOP-92	1.15	1.44	1.94	1.58	OVCAR-5	2.46	**2.44**	**2.12**	3.16
NCI-H226	2.69	**1.73**	**1.45**	2.00	OVCAR-8	2.34	2.63	**2.11**	2.51
NCI-H23	2.48	**1.70**	**1.83**	2.00	ADR-RES	2.43	**2.07**	**1.95**	2.51
NCI-H322M	2.62	**2.33**	**2.24**	2.51	SK-OV-3	1.89	2.18	**1.82**	2.51
NCI-H460	1.79	2.01	1.91	2.51	**Renal Cancer**				
NCI-H522	2.54	**1.97**	**1.66**	2.00	786-0	1.79	2.22	**1.03**	3.16
Colon Cancer					A498	2.49	**1.90**	**1.83**	2.51
COLO 205	ND[c]	2.10	1.80	2.00	ACHN	1.85	**1.68**	**1.39**	2.51
HCC-2998	ND[c]	3.00	2.05	3.16	CAKI-1	2.54	**2.05**	**1.94**	3.16
HCT-116	1.89	**1.78**	**1.73**	1.58	RXF 393	1.93	**1.81**	**1.67**	3.16
HCT-15	1.95	2.09	**1.65**	2.51	SN12C	2.44	2.58	**1.80**	2.51
HT29	ND[c]	2.14	**1.27**	2.00	TK-10	2.29	4.45	2.50	3.98
KM12	3.41	***0.446***	***0.019***	1.58	UO-31	2.17	**1.65**	**1.83**	2.51
SW-620	2.99	3.31	**2.07**	2.51	**Prostate Cancer**				
CNS Cancer					PC-3	1.42	2.04	1.87	2.00
SF-268	2.34	3.22	**2.00**	2.51	DU-145	2.24	2.73	**1.76**	3.16
SF-295	1.79	1.90	**1.82**	1.58	**Breast Cancer**				
SF-539	1.78	**1.58**	**1.54**	1.58	MCF7	1.72	1.75	**1.23**	2.51
SNB-19	2.77	3.82	**2.33**	3.16	MDA-MB-231	1.43	2.14	1.74	1.26
SNB-75	1.52	1.74	**1.37**	3.16	HS 578T	1.53	2.55	2.01	2.51
U251	1.79	**1.77**	1.85	2.00	BT-549	2.64	3.02	**2.32**	3.16
Melanoma					T-47D	0.72	1.53	1.99	1.58
LOX IMVI	2.68	**1.82**	**1.71**	1.58	MDA-MB-468	1.36	1.45	1.66	2.00
MALME-3 M	1.61	**1.44**	**1.20**	2.00					

[a] Data were obtained from the NCI in vitro disease-oriented human tumor cell line screen (five-dose–response curve). [b] Bold figures refer to superior potency over the lead candidate **A**, bold italicized figures indicate sub-micromolar GI_{50} values for **5** and **6**. [c] Not determined.

of compound **6** was demonstrated by its ability to trigger total growth inhibition (TGI, Zero growth) in relatively small doses (TGI < 5.0 μM) than compound **A** and sorafenib over multiple cell lines. For example, the leukemia SR cell line (**6**, TGI = 0.846 μM; **A**, TGI = 9.10 μM; sorafenib, TGI = 100 μM). The ethylpiperazine compound **6** was also able to induce 50% tumor regression (LC_{50}, 50% lethality) against numerous cell lines with LC_{50} values < 10.0 μM.

Furthermore, the cytotoxicity of compound **6** has been examined against the human foreskin fibroblast (HFF-1) normal cell line using 3-(4,5-dimethylthiazol-2-yl)-2,5-diphenyltetrazolium bromide (MTT) assay. At 1.0 μM concentration, which is close to the mean GI_{50} value over NCI-60 cancer cells, compound **6** showed low growth inhibitory activity (10.36 ± 0.19% inhibition) against HFF-1 normal cell. Such finding may reveal the differential cytotoxic activity of compound **6** toward human cancer cells rather normal cell lines.

Encouraged by the promising cellular potency of the ethylpiperazine derivative **6** and with the goal of investigating the kinase inhibitory profile, it was tested over a panel of 50 oncogenic kinases at 10 μM concentration at Reaction Biology Corporation (RBC, USA).[22] As illustrated in Table 4, compound **6** potently inhibited 23 kinases by more than 90%. For example, ABL-1 (93.7%), LYN (99.6%), DDR1 (98.8%), FLT3 (96.8%), RET (97%) and RAF1 (98.3%). Such findings disclose the distinct multiple kinase inhibitory effect of compound **6** toward the different classes of kinases, particularly the tyrosine protein kinases (TKs). Relatively, the cyclin dependent kinase family (CMGC) members, like JNK1, JNK3, and MAPK13 were moderately inhibited by **6**. Because those kinases inhibited by **6** are involved in different cellular signaling pathways for tumorigenesis (such as Ras/Raf/Mek/Erk)[23] and angiogenesis (such as VEGF),[24] it could be concluded that compound **6** may exert its broad spectrum anticancer activity via multiple mechanism of actions.

To further examine the potency of compound **6**, its IC_{50} values were determined against a selected array (14 kinases) of the most important kinases implicated in cancer pathogenesis (Table 5). With the goal of comparative study, the lead compound **A** was tested for its inhibitory activity over certain sensi-

Table 3. TGI and LC_{50} [μM] values of compounds **A**, **5**, **6** and sorafenib over a selected array of sensitive cell lines.[a,b]

Cell line	A		5		6		Sorafenib	
	TGI	LC_{50}	TGI	LC_{50}	TGI	LC_{50}	TGI	LC_{50}
Leukemia								
CCRF-CEM	>100	>100	>100	>100	**2.47**	*61.0*	100	100
K-562	>100	>100	>100	>100	**1.27**	*6.90*	100	100
SR	9.10	>100	ND[c]	>100	**0.846**	*46.6*	100	100
NSCL Cancer								
NCI-H226	7.47	>100	**4.30**	*12.8*	**3.16**	*6.91*	7.94	31.6
NCI-H522	>100	>100	**8.36**	*62.9*	**3.59**	*7.67*	6.31	25.1
Colon Cancer								
HCT-116	5.39	>100	**3.63**	*7.39*	**3.45**	*6.86*	3.98	15.9
KM12	>100	>100	**2.31**	*17.0*	**1.63**	*5.63*	7.94	31.6
CNS Cancer								
SF-539	3.90	ND[c]	**3.37**	7.22	**2.97**	*5.73*	10.0	50.1
SNB-75	3.24	6.88	**4.95**	21.9	**2.73**	*5.46*	10.0	39.8
Melanoma								
LOX IMVI	>100	>100	**4.34**	*13.4*	**3.17**	*5.85*	3.16	7.94
UACC-257	>100	>100	**5.59**	*20.0*	**3.51**	*6.64*	5.01	20.0
Renal Cancer								
A498	12.2	>100	**4.05**	*8.65*	**3.54**	*6.87*	6.31	31.6
SN12C	>100	>100	**9.36**	*67.8*	**3.66**	*7.43*	10.0	39.8
Breast Cancer								
MDA-MB-231	4.29	59.2	5.80	*45.9*	**3.40**	*6.65*	3.98	20.0
BT-549	9.73	>100	**9.18**	*36.3*	**4.25**	*7.79*	5.01	15.8

[a] Data were obtained from the NCI in vitro disease-oriented human tumor cell line screen (five-dose–response curve). [b] Bold figures and italicized figures refer to superior efficacies over the lead candidate **A** in terms of TGI and LC_{50} values, respectively. [c] Not determined.

Table 4. Percent inhibition exerted by compound **6** over a panel of 50 oncogenic kinases at a concentration of 10 μM.[a]

Kinase class/name	Inhibition [%]	Kinase class/name	Inhibition [%]
Non-receptor tyrosine kinase		PDGFRα	97.3
ABL1	93.7	RET	97.0
$ABL1^{T315I}$	93.1	TIE2	98.5
ABL2	83.1	TRKA	98.3
BMX	75.0	TRKB	98.4
CSK	84.6	**Serine/threonine kinases**	
c-Src	67.4	Aurora A	27.5
FAK	18.3	MAP4K2	48.5
FER	88.4	LCK2	−87.2
FES	90.0	LOK	88.0
FYN	95.3	PIM1	14.4
JAK1	56.5	PIM2	1.4
LCK	98.5	SGK1	14.0
YES	93.6	TAK1	90.7
LYN	99.6	TNIK	90.3
Receptor tyrosine kinase		ZAK	87.0
ALK	15.7	**Tyrosine kinase like kinases (TKL)**	
c-MET	26.2	BRAF	71.4
DDR1	98.8	$BRAF^{V600E}$	95.2
DDR2	91.6	RAF1	98.3
EGFR	30.1	**CMGC group**[b]	
EPHA2	97.8	JNK1	66.5
EPHA3	97.7	JNK2	83.5
FLT3	96.8	JNK3	60.1
FMS	90.4	MAPK12	79.4
FGFR3	82.7	MAPK13	44.3
VEGFR1	98.3	MAPK14	87.8
VEGFR2	98.9		

[a] Compound **6** was tested in single-dose duplicate mode at a concentration of 10 μM. [b] CMGC: cyclin-dependent kinase family.

tive kinases potently inhibited by compound **6**, and sorafenib was used as a reference compound.

As shown in Table 5, compound **6** showed an equipotent activity against both the wild-type ABL kinase (IC_{50} = 52.7 nM) and its most resistant gatekeeper mutant ABL^{T315I} (IC_{50} = 53.3 nM), while sorafenib was less active (ABL-1, IC_{50} = 1133 nM; ABL^{T315I} IC_{50} = 957 nM) and the lead compound **A** was quite inactive (IC_{50} > 10 μM). ABL generated by BCR-ABL fusion is a non-receptor TK, and its constitutive activation is known to be the etiologic cause for chronic myeloid leukemia (CML).[27] In this regard, it is noteworthy mentioning that compound **6** exerted a magnificent anticancer activity against the ABL dependent leukemia K-562 cell line with GI_{50} value of 51.4 nM.

c-Src family kinases (SFK), like c-Src, FYN, LYN, YES and LCK, are cytoplasmic TKs which possess a high degree of structural similarity to ABL. While the chloro compound **A** showed an unpretentious activity against LCK and LYN kinases (IC_{50} > 10 μM), its corresponding ethylpiperazine **6** displayed a potent inhibitory activity surpassing sorafenib over certain SFK members, such as LCK (IC_{50} = 6.66 nM), LYN (IC_{50} = 19.9 nM), and FYN (IC_{50} = 160 nM).

Apart from the cytoplasmic TKs, the discoidin domain containing receptor (DDR1) is a receptor TK whose deregulation is associated with the progression of breast,[28] and colon[29] cancers. Interestingly, compound **6** was able to inhibit the DDR1 kinase on the enzymatic level (IC_{50} = 26.5 nM), being sixfold

Table 5. IC_{50} values of compounds **6**, **A**, and sorafenib against the most sensitive kinases.[a,b]

Kinase	**6**		**A**		Sorafenib
	Inhibition [%]	IC_{50} [nM]	Inhibition [%]	IC_{50} [nM]	IC_{50} [nM]
ABL1	93.7	**52.7**	31.3	>10000	1133[25]
ABL^{T315I}	93.1	**53.3**	NT	NT	957[25]
$BRAF^{V600E}$	71.4	133	NT	NT	38.0[10]
DDR1	98.8	**26.5**	87.9	NT	160[26]
VEGFR1	98.3	**42.8**	−3	>10000	26.0[10]
VEGFR2	98.9	**43.1**	22.6	>10000	90.0[10]
LCK	98.5	**6.66**	31	>10000	1495[25]
LYN	99.6	**19.9**	12	>10000	510[26]
RAF1	98.3	**61.7**	94.8	111	6.0[10]
TrkA	98.3	**3.81**	−0.2	>10000	218[25]
TrkB	98.4	**4.42**	NT	NT	832[25]
Tie2	98.5	**0.82**	7.0	>10000	–
FMS	90.4	102	NT	NT	29.0[25]
FYN	95.3	160	NT	NT	–

[a] Compound **6** was tested in a 10-dose IC_{50} mode with 3-fold serial dilution starting at 20 μM; NT: not tested [b] Bold figures refer to potent activity (sub-nanomolar, single- or double-digit nanomolar IC_{50} values).

more potent than sorafenib (IC_{50} = 160 nM). In addition, it showed anticancer activity against the DDR1 relevant cell lines (colon HCT-116, GI_{50} = 1.73 μM; breast T-47D, GI_{50} = 1.99 μM). Also, the lead compound **A** showed a considerable activity toward DDR1 kinase (88% inhibition at 10 μM).

By referring to the angiogenesis mediating kinases, VEGFR,[24] it is interesting to report the equipotent activity of compound **6** over both VEGFR1 and VEGFR2 (IC_{50} = 43 nM). Most importantly, Tie2 kinase, the other key regulator for tumor angiogenesis,[30] was potently suppressed by compound **6** (IC_{50} = 0.82 nM). Such promising biochemical results of compound **6** provide a strong evidence for its prospective anti-angiogenic activity. In contrast, the lead compound **A** was extremely inactive (IC_{50} > 10 μM) against VEGFR1, VEGFR2, and Tie2 kinases, while sorafenib was relatively more potent toward VEGFR1 (IC_{50} = 26 nM) than VEGFR2 kinase (IC_{50} = 90 nM).

On the other hand, tropomyosin related kinases (Trk) are receptor TKs for the neurotrophin family of ligands that play a pivotal role for growth and differentiation in normal neuronal cells.[31] Pathological overexpression of TrkA is linked to malignant transformation and invasion signaling in certain human cancers including breast,[32] colon,[33] and neuroblastoma.[34] Moreover, the overexpression of TrkB has been reported in various malignancies.[35] In this sense, compound **6** showed a distinct inhibitory effects against both TrkA (IC_{50} = 3.81 nM) and TrkB (IC_{50} = 4.42 nM). Such great activity was also observed on the TrkA relevant colorectal KM12 cell line[36] (GI_{50} = 19 nM).

In respect to the tyrosine kinase like (TKL) kinases, exemplified by RAF kinases, both compounds **A** and **6** showed favorable inhibitory effects (**A**, IC_{50} = 111 nM; **6**, IC_{50} = 61.7 nM) against C-RAF (RAF1) kinase. In comparison with sorafenib (IC_{50} = 6.0 nM), both compounds **A** and **6** were relatively less potent. C-RAF kinase is implicated in the abnormal proliferation in melanoma[37] as well as being overexpressed in renal cell carcinoma (RCC),[38] and colon cancers.[39] The nanomolar activity of compound **6** over C-RAF kinase suggest its possible effects on the Ras/Raf/Mek/Erk pathway.

Based on the aforementioned findings, we can conclude that both compounds **A** and **6** are able to target the DDR1 and RAF kinases. Moreover, replacing the small chlorine atom of the lead compound **A** with (4-ethylpiperazin-1-yl)methyl moiety has resulted in a substantial kinase inhibitory activity toward a number of oncogenic kinases which could not be inhibited by the original lead **A**.

To better understand and justify the obtained kinase inhibitory activities of both compounds **A** and **6** from a 3D structural perspective, a molecular docking study was conducted. Firstly, we aimed at addressing the binding affinity of compounds **A** and **6** toward the DDR1 kinase (PDB ID: 4CKR).[40] As illustrated in Figure 3, both compounds **A** and **6** are well bound into the ATP binding site of DDR1 kinase through forming the crucial hydrogen bond (HB) with the Met704 residue in the kinase hinge region via their pyridine nitrogen. Moreover, the urea moiety of benzothiazoles was engaged in three additional HBs with Asp784 and Glu672. In addition, the *m*-trifluoromethylphenyl group of compounds **A** and **6** was involved in hydrophobic interactions with the backbone Asp784 residue in the DFG region. An additional ionic interaction was observed between the positively charged nitrogen of ethylpiperazine in compound **6** and the negatively charged carbonyl oxygen of Asp784, which may explain the superior binding affinity of **6** (Gscore = −11.972 kcal mol^{-1}) rather the chloro compound **A** (Gscore = −10.418 kcal mol^{-1}).

Secondly, we focused our efforts to recognize the significant role of (4-ethylpiperazin-1-yl)methyl moiety in compound **6** for targeting certain kinases not inhibited by the original lead **A**, like VEGFR2, LYN, TrkA and Tie2. Therefore, a molecular docking study for both compounds **A** and **6** was performed using the crystal structures of VEGFR2[41] and TrkA[42] as representative examples. Inspection of the predicted binding modes of compounds **A** and **6** in VEGFR2[41] (Figure 4) revealed that both compounds could contribute in significant binding interactions

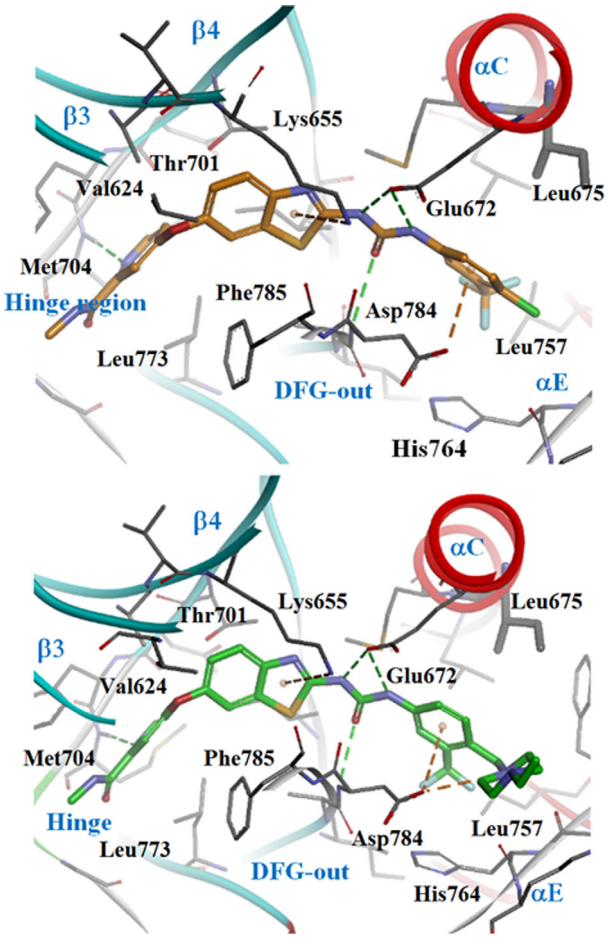

Figure 3. The predicted binding mode of compounds **A** (orange, top) and **6** (green, bottom) in the catalytic kinase domain of DDR1 in its DFG-out conformation.

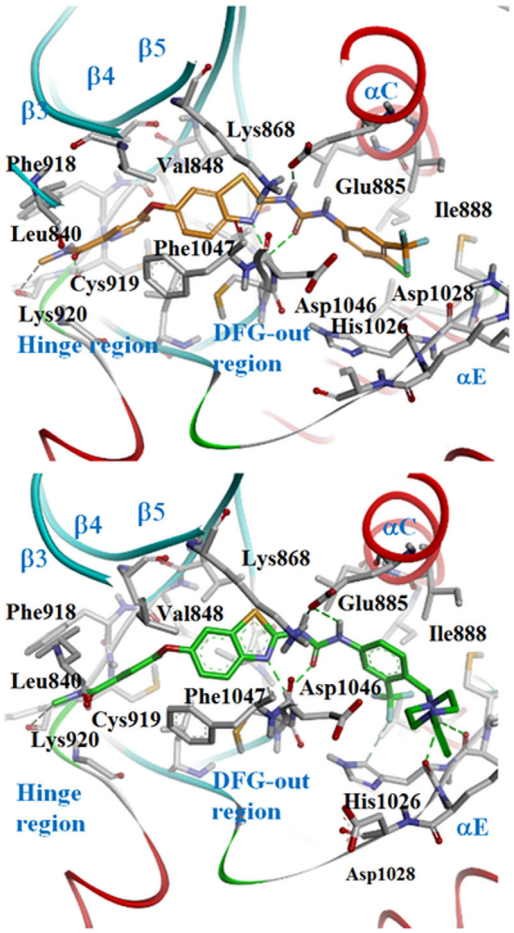

Figure 4. The putative binding mode of compounds **A** (orange, top) and **6** (green, bottom) in the catalytic kinase domain of VEGFR2 in its DFG-out conformation.

with the hinge region residue (Cys919) via their *N*-methylpicolinamide head, DFG loop (Asp1046) and C-helix (Glu885) residues through their urea spacer, and hydrophobic pocket via their *m*-trifluoromethylphenyl moiety. However, only compound **6** was able to access the deep hydrophobic pocket in the VEGFR2 allosteric site through its piperazinyl group, which is expected to create bifurcated hydrogen bonds with the backbone -CO groups of VEGFR2 residues (His1026). These interactions are in accordance with those observed in several crystal structures of type II kinase inhibitors and could provide a logical justification for the superior potency of compound **6** than its original lead **A** toward VEGFR2.

On the other hand, regarding TrkA kinase, the putative binding mode illustrated in Figure 5 revealed that both compounds **A** and **6** lacked HB interactions with Met592 in the TrkA hinge region. However, this deficiency in hinge region binding was compensated, in compound **6**, by the significant hydrophobic interactions between its ethylpiperazinyl moiety and the allosteric binding site around α-C segment of TrkA kinase. The ethylpiperazinyl group is expected to be deeply inserted within the hydrophobic pocket (Phe646 and His648) adjacent to the ATP binding site, in addition to the formation of HB with Asp668 and hence increasing the binding affinity of compound **6** with TrkA. The missing of such hydrophobic and HB interaction in the original lead **A** could explain its low TrkA inhibitory activity. Taken together, we can conclude that the insertion of (4-ethylpiperazin-1-yl)methyl moiety instead of chlorine in compound **A** plays an important role in increasing the binding affinity toward multiple oncogenic kinases. Moreover, the putative binding modes of compound **6** suggest its possibility to be a type II kinase inhibitor.

Furthermore, the in vivo pharmacokinetic (PK) properties of compound **6** was evaluated (Table 6). The AUC_{∞} values of compound **6** are 4.24 μg h mL^{-1} and 1.07 μg h mL^{-1} in intravenous and oral administration, respectively. Compound **6** was slowly distributed to reach the blood after oral administration (t_{max} = 4.67 h), and exhibited slow clearance (21 mL kg^{-1} min^{-1}). In addition, it showed good oral exposure as indicated by its C_{max} value (64.6 ng mL^{-1}). Taken together, compound **6** possesses a favorable PK properties with reasonable oral bioavailability (*F*) value of 25.1 %.

In conclusion, a new potent benzothiazole multikinase inhibitor **6** (KST016366) has been discovered, through changing the hydrophobic tail of our previously reported RAF kinase inhibitor **A**. The ethylpiperazinyl derivative **6** exerted broad spectrum antiproliferative activity against NCI-60 cancer cell lines,

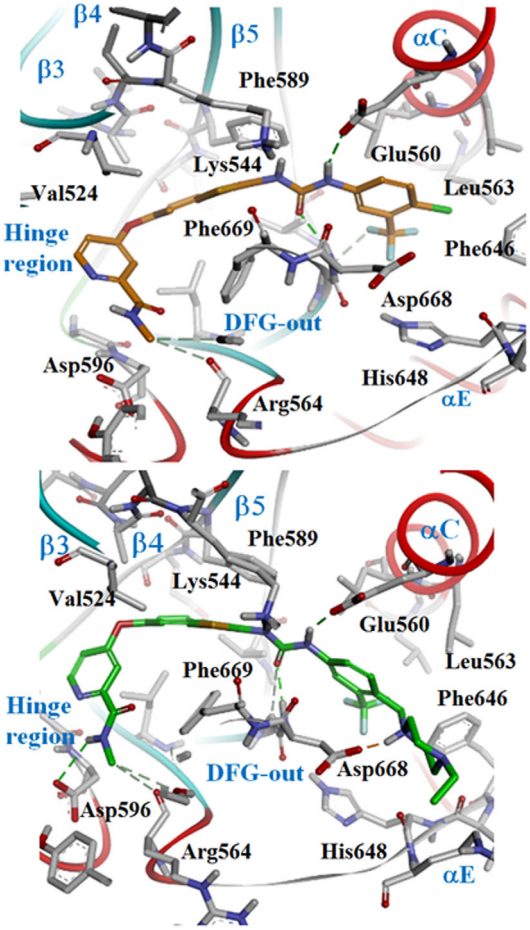

Figure 5. The predicted binding mode of compounds **A** (orange, top) and **6** (green, bottom) in the catalytic kinase domain of TrkA in its DFG-out conformation.

Table 6. Mean PK of compound **6** following intravenous (i.v.) or oral (p.o.) dosing in male rats.[a,b]

Parameter	i.v.	p.o.
t_{max} [h]	–[b]	4.67 ± 1.15
C_{max} [ng mL^{-1}]	–[b]	64.6 ± 0.0124
$t_{1/2}$ [h]	4.52 ± 1.09	11.4 ± 6.98
AUC_t [μg h mL^{-1}]	4.14 ± 1.39	0.704 ± 0.392
AUC_t [μg h mL^{-1}]	4.24 ± 1.5	1.07 ± 0.893
CL [mL kg^{-1} min^{-1}]	21.0 ± 0.445	–[b]
V_{ss} [L kg^{-1}]	6.97 ± 1.84	–[b]
F [%]		25.1

[a] Dosed at 5 mg kg^{-1}; values are the mean ± SD (n = 3). AUC: area under plasma concentration time curve; C_{max}: peak plasma concentration; t_{max}: time to reach C_{max}; CL: body clearance; F: oral bioavailability. [b] Not determined.

particularly over the leukemia K-562 and colorectal KM12 cell lines with nanomolar GI_{50} values. Moreover, KST016366 showed potent inhibitory effects over certain oncogenic kinases like Tie2, LCK, TrkA, wild-type and T315I mutant ABL. Molecular docking study of KST016366 provided some insight about the role of (4-ethylpiperazin-1-yl)methyl-3-trifluoromethylphenyl moiety in targeting multiple oncogenic kinases. Also, KST016366 showed favorable PK profile with good oral bioavailability. Therefore, KST016366 could be considered as a promising candidate for further preclinical and clinical investigations or a lead compound for development of potent anticancer chemotherapeutics.

Acknowledgements

This research was supported by the Korea Institute of Science and Technology (KIST) Institutional Program (2E26650 and 2E26663). We express our sincere appreciation and gratitude to the National Cancer Institute (NCI, Bethesda, MD, USA) for performing the anticancer evaluation of the new compounds.

Keywords: anticancer activity · benzothiazoles · ethylpiperazine · multikinase inhibitors

[1] *World Cancer Report 2014* (Eds.: B. W. Stewart, C. W. Wild), International Agency for Research on Cancer (IARC), Lyon, France, **2014**; https://shop.iarc.fr/products/wcr2014 [ISBN (PDF): 978-92-832-0443-5; ISBN (EPUB): 978-92-832-0432-9].
[2] K. S. Kolibaba, B. J. Druker, *Biochim. Biophys. Acta Rev. Cancer* **1997**, *1333*, F217 – F248.
[3] J. E. Dancey, H. X. Chen, *Nat. Rev. Drug Discovery* **2006**, *5*, 649 – 659.
[4] L. Gossage, T. Eisen, *Clin. Cancer Res.* **2010**, *16*, 1973 – 1978.
[5] H. Daub, K. Specht, A. Ullrich, *Nat. Rev. Drug Discovery* **2004**, *3*, 1001 – 1010.
[6] V. von Manstein, C. M. Yang, D. Richter, N. Delis, V. Vafaizadeh, B. Groner, *Curr. Signal Transduction Ther.* **2013**, *8*, 193 – 202.
[7] S. Giordano, A. Petrelli, *Curr. Med. Chem.* **2008**, *15*, 422 – 432.
[8] A. D. Boran, R. Iyengar, *Curr. Opin. Drug Discovery Dev.* **2010**, *13*, 297 – 309.
[9] Z. Zhao, H. Wu, L. Wang, Y. Liu, S. Knapp, Q. Liu, N. S. Gray, *ACS Chem. Biol.* **2014**, *9*, 1230 – 1241.
[10] S. Wilhelm, C. Carter, M. Lynch, T. Lowinger, J. Dumas, R. A. Smith, B. Schwartz, R. Simantov, S. Kelley, *Nat. Rev. Drug Discovery* **2006**, *5*, 835 – 844.
[11] P. T. Wan, M. J. Garnett, S. M. Roe, S. Lee, D. Niculescu-Duvaz, V. M. Good, C. G. Project, C. M. Jones, C. J. Marshall, C. J. Springer, D. Barford, R. Marais, *Cell* **2004**, *116*, 855 – 867.
[12] T. O'Hare, W. C. Shakespeare, X. Zhu, C. A. Eide, V. M. Rivera, F. Wang, L. T. Adrian, T. Zhou, W.-S. Huang, Q. Xu, C. A. Metcalf III, J. W. Tyner, M. M. Loriaux, A. S. Corbin, S. Wardwell, Y. Ning, J. A. Keats, Y. Wang, R. Sundaramoorthi, M. Thomas, D. Zhou, J. Snodgrass, L. Commodore, T. K. Sawyer, D. C. Dalgarno, M. W. Deininger, B. J. Druker, T. Clackson, *Cancer Cell* **2009**, *16*, 401 – 412.
[13] K. S. Gajiwala, J. C. Wu, J. Christensen, G. D. Deshmukh, W. Diehl, J. P. DiNitto, J. M. English, M. J. Greig, Y.-A. He, S. L. Jacques, E. A. Lunney, M. McTigue, D. Molina, T. Quenzer, P. A. Wells, X. Yu, Y. Zhang, A. Zou, M. R. Emmett, A. G. Marshall, H.-M. Zhange, G. D. Demetrih, *Proc. Natl. Acad. Sci. USA* **2009**, *106*, 1542 – 1547.
[14] Y. Liu, N. S. Gray, *Nat. Chem. Biol.* **2006**, *2*, 358 – 364.
[15] L. Tan, T. Nomanbhoy, D. Gurbani, M. Patricelli, J. Hunter, J. Geng, L. Herhaus, J. Zhang, E. Pauls, Y. Ham, H. G. Choi, T. Xie, X. Deng, S. J. Buhrlage, T. Sim, P. Cohen, G. Sapkota, K. D. Westover, N. S. Gray, *J. Med. Chem.* **2015**, *58*, 183 – 196.
[16] A. K. El-Damasy, S. H. Seo, N.-C. Cho, S. B. Kang, A. N. Pae, K.-S. Kim, G. Keum, *Eur. J. Med. Chem.* **2015**, *101*, 754 – 768.
[17] A. K. El-Damasy, J.-H. Lee, S. H. Seo, N.-C. Cho, A. N. Pae, G. Keum, *Eur. J. Med. Chem.* **2016**, *115*, 201 – 216.
[18] A. K. El-Damasy, N.-C. Cho, S. B. Kang, A. N. Pae, G. Keum, *Bioorg. Med. Chem. Lett.* **2015**, *25*, 2162 – 2168.
[19] W. Shen, M. S. Tremblay, V. A. Deshmukh, W. Wang, C. M. Filippi, G. Harb, Y.-q. Zhang, A. Kamireddy, J. E. Baaten, Q. Jin, T. Wu, J. G. Swoboda, C. Y. Cho, J. Li, B. A. Laffitte, P. McNamara, R. Glynne, X. Wu, A. E. Herman, P. G. Schultz, *J. Am. Chem. Soc.* **2013**, *135*, 1669 – 1672.

[20] NCI, Division of Cancer Treatment & Diagnosis, Developmental Therapeutics Program (DTP): https://dtp.cancer.gov/.
[21] DTP Data Search: https://dtp.cancer.gov/dtpstandard/dwindex/index.jsp (retrieved May 24, 2016).
[22] Reaction Biology Corp.: www.reactionbiology.com.
[23] H. Rajagopalan, A. Bardelli, C. Lengauer, K. W. Kinzler, B. Vogelstein, V. E. Velculescu, *Nature* **2002**, *418*, 934 – 934.
[24] A. Hoeben, B. Landuyt, M. S. Highley, H. Wildiers, A. T. Van Oosterom, E. A. De Bruijn, *Pharmacol. Rev.* **2004**, *56*, 549 – 580.
[25] R. Kumar, M. C. Crouthamel, D. H. Rominger, R. R. Gontarek, P. J. Tummino, R. A. Levin, A. G. King, *Br. J. Cancer* **2009**, *101*, 1717 – 1723.
[26] D. Kitagawa, K. Yokota, M. Gouda, Y. Narumi, H. Ohmoto, E. Nishiwaki, K. Akita, Y. Kirii, *Genes Cells* **2013**, *18*, 110 – 122.
[27] M. W. Deininger, J. M. Goldman, J. V. Melo, *Blood* **2000**, *96*, 3343 – 3356.
[28] K. A. Toy, R. R. Valiathan, F. Núñez, K. M. Kidwell, M. E. Gonzalez, R. Fridman, C. G. Kleer, *Breast Cancer Res. Treat.* **2015**, *150*, 9 – 18.
[29] R. R. Valiathan, M. Marco, B. Leitinger, C. G. Kleer, R. Fridman, *Cancer Metastasis Rev.* **2012**, *31*, 295 – 321.
[30] N. Jones, K. Iljin, D. J. Dumont, K. Alitalo, *Nat. Rev. Mol. Cell Biol.* **2001**, *2*, 257 – 267.
[31] S. D. Skaper, *CNS Neurol. Disord. Drug Targets* **2008**, *7*, 46 – 62.
[32] E. Adriaenssens, E. Vanhecke, P. Saule, A. Mougel, A. Page, R. Romon, V. Nurcombe, X. Le Bourhis, H. Hondermarck, *Cancer Res.* **2008**, *68*, 346 – 351.
[33] A. Nakagawara, *Cancer Lett.* **2001**, *169*, 107 – 114.
[34] G. M. Brodeur, J. E. Minturn, R. Ho, A. M. Simpson, R. Iyer, C. R. Varela, J. E. Light, V. Kolla, A. E. Evans, *Clin. Cancer Res.* **2009**, *15*, 3244 – 3250.
[35] Y. Yu, S. Zhang, X. Wang, Z. Yang, G. Ou, *APMIS* **2010**, *118*, 188 – 195.
[36] E. Ardini, R. Bosotti, A. L. Borgia, C. De Ponti, A. Somaschini, R. Cammarota, N. Amboldi, L. Raddrizzani, A. Milani, P. Magnaghi, D. Ballinari, D. Casero, F. Gasparri, P. Banfi, N. Avanzi, M. B. Saccardo, R. Alzani, T. Bandiera, E. Felder, D. Donati, E. Pesenti, A. Sartore-Bianchi, M. Gambacorta, M. A. Pierotti, S. Siena, S. Veronese, A. Galvani, A. Isacchi, *Mol. Oncol.* **2014**, *8*, 1495 – 1507.
[37] L. B. Jilaveanu, C. R. Zito, S. A. Aziz, P. J. Conrad, J. C. Schmitz, M. Sznol, R. L. Camp, D. L. Rimm, H. M. Kluger, *Clin. Cancer Res.* **2009**, *15*, 5704 – 5713.
[38] H. Oka, Y. Chatani, R. Hoshino, O. Ogawa, Y. Kakehi, T. Terachi, Y. Okada, M. Kawaichi, M. Kohno, O. Yoshida, *Cancer Res.* **1995**, *55*, 4182 – 4187.
[39] J. Y. Fang, B. C. Richardson, *Lancet Oncol.* **2005**, *6*, 322 – 327.
[40] H.-G. Kim, L. Tan, E. L. Weisberg, F. Liu, P. Canning, H. G. Choi, S. A. Ezell, H. Wu, Z. Zhao, J. Wang, A. Mandinova, J. D. Griffin, A. N. Bullock, Q. Liu, S. W. Lee, N. S. Gray, *ACS Chem. Biol.* **2013**, *8*, 2145 – 2150.
[41] K. Okamoto, M. Ikemori-Kawada, A. Jestel, K. von König, Y. Funahashi, T. Matsushima, A. Tsuruoka, A. Inoue, J. Matsui, *ACS Med. Chem. Lett.* **2015**, *6*, 89 – 94.
[42] S. J. Stachel, J. M. Sanders, D. A. Henze, M. T. Rudd, H.-P. Su, Y. Li, K. K. Nanda, M. S. Egbertson, P. J. Manley, K. L. Jones, E. J. Brnardic, A. Green, J. A. Grobler, B. Hanney, M. Leitl, M.-T. Lai, V. Munshi, D. Murphy, K. Rickert, D. Riley, A. Krasowska-Zoladek, C. Daley, P. Zuck, S. A. Kane, M. T. Bilodeau, *J. Med. Chem.* **2014**, *57*, 5800 – 5816.

Received: April 26, 2016
Revised: May 25, 2016
Published online on ■■ ■■, 0000

These are not the final page numbers! ↗↗

COMMUNICATIONS

*A. K. El-Damasy, N.-C. Cho, G. Nam, A. N. Pae, G. Keum**

■■ – ■■

Discovery of a Nanomolar Multikinase Inhibitor (KST016366): A New Benzothiazole Derivative with Remarkable Broad-Spectrum Antiproliferative Activity

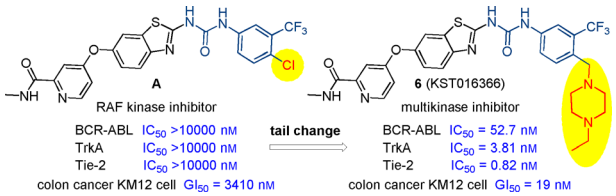

A potent oral multikinase inhibitor was identified: KST016366. Slight modification of the hydrophobic tail of RAF kinase inhibitor **A** has a dramatic impact on cellular and enzymatic activity. KST016366 exerts distinct inhibitory effects on multiple oncogenic kinases, in contrast to its lead compound **A**. KST016366 shows nanomolar antiproliferative activity against both leukemia K-562 (ABL-kinase-dependent) and colon carcinoma KM12 (TrkA-dependent) cells. Moreover, KST016366 inhibits two key angiogenic kinases: VEGFR2 and Tie2.